Theor Chim Acta (1995) 91: 215–224

Theoretica Chimica Acta

Density-functional investigation of the excited state properties and the Jahn–Teller effect in $[CrX6]^{3-}$ ($X = Cl^-$, Br^-)

Khalid Bellafrouh[1], Claude Daul[1], Hans U. Güdel[2], François Gilardoni[3], Jacques Weber[3]

[1] Institut de Chimie Inorganique et Analytique, Université de Fribourg, CH-1700 Fribourg, Suisse

[2] Institut für Anorganische, Analytische Chemie, Universität Bern, Freiestrasse 3, CH-3000 Bern 9, Switzerland

[3] Département de Chimie Physique, Université de Genève, CH-1211 Genève 4, Suisse

Received June 8, 1994/Final revision received October 18, 1994/Accepted October 20, 1994

Summary. The luminescence of $[CrX_6]^{3-}$ $X = Br^-$, Cl^- has been studied through density functional theory (DFT) using both deMon and ADF codes. Multiplet energies $^4A_2$, ^2E, $^4T_2$, and $^4T_1$ have been expressed as energies of non-redundant single determinants and calculated as in Ref. [1]. The influence of the metal ligand distance on the multiplet energies has been investigated. Of particular interest to this work is the Jahn–Teller effect distortion. We found that the system moves to a more stable geometry when the axial bond length is compressed and the equatorial one elongated in agreement with the experimental value.

Key words: Density functional theory – Excited states – Jahn–Teller effect

1 Introduction

The accurate calculation of the electronic structure of transition metal complexes still remains a major challenge to quantum chemistry. In order to interpret absorption and fluorescence spectra, the multiple scattering (MS) local spin density (LSD) method was used in previous investigations to obtain the monoelectronic energies of octahedral complexes, e.g. $[CrO_6]^{3-}$ and $[MnF_6]^{4-}$ [2, 3]. Thus, the e_g and t_{2g} wave functions were used to compute the Racah parameters B and C [4] and the Slater transition state theory [5] to evaluate the 10Dq crystal field parameter. These values were then used in a ligand field (LF) model to calculate the LF state energies.

In this paper we investigate the excited state properties and then Jahn–Teller effect in $[CrX_6]^{3-}$ ($X = Br^-$, Cl^-) through DFT. Some Cr^{3+} doped elpasolites Cs_2NaMX_6 ($M = In, Y$; $X = Cl, Br$) are promising candidates for solid state laser action [6]. They provide excellent hosts for the study of lattices for the study of Cr^{3+} in low crystal fields. Their space groups are cubic and the site symmetry at the metal position (M^{3+}) is O_h. Ion Cr^{3+} has a high luminescent quantum efficiency as a dopant in the title materials at low temperature [7, 8].

Recent publications have shown that when the *ab initio* method at the Hartee–Fock (HF) level or with limited CI is used for such studies, the results of these calculations yield only very qualitative information [9–12]. Based on the HF

approach, calculations on small transition metal systems like $[CrF_6]^{3-}$ have indicated that very elaborate wave functions are most often necessary in order to obtain a quantitative description of spectroscopic properties [13]. Clearly, an extensive treatment of electron correlations is needed if one wants to obtain more accurate results [14, 15].

On the other hand, when using the DFT method, correlation is partly taken in to account, considering the functional form of the exchange correlation contribution. We will show in this paper that we reach the same precision as that obtained using more time-consuming methods, including CASSCF, for the calculation of multiplet structures.

Another important result of this study deals with the Jahn–Teller distortion [16] of the luminescent $^4T_2$ state. We will show that the predicted tetragonal distortion of the title compounds resulting from the vibronic coupling of the $^4T_2$ with an e_g-mode is in agreement with the observed one.

2 Computational methods

2.1 Density functional calculations

Both the linear combination of Gaussian type orbital–model core potential–density functional (LCGTO-MCP-DF) method [17–20] and its corresponding deMon program package developed by the group of Salahub, and Hartree–Fock–Slater–linear combination of atomic orbitals (HFS-LCAO) as implemented in the Amsterdam density functional (ADF) program system developed by Baerends et al. [21–24] have been used.

All the calculations reported in this study were performed using the Vosko–Wilk–Nusair (VWN) exchange-correlation potential [25] augmented by nonlocal gradient corrections as suggested by Becke for exchange functional and Perdew for correlation (BP) [26–28].

In the deMon calculations, all the core and valence electrons were explicitly taken into account, whereas the frozen core option was applied when ADF was used.

The one-electron (orbital) basis set used in the deMon calculations has been optimised for LCGTO-DF calculations by Godbout and Andzelm [29]. In this case, the Cr, Cl and Br basis sets are of double zeta plus polarisation quality, the contraction patterns being Cr(63321/5211/41), Cl(7321/621/1), Br(63321/5321/41), which leads in the usual six-component d-type Cartesian Gaussian functions to a basis set of dimension 143 for $[CrCl_6]^{3-}$ and dimension 203 for $[CrBr_6]^{3-}$. The auxiliary basis sets required by the LCGTO-DF model to fit the electron density and the exchange-correlation potential have been chosen as Cr(5,5;5,5), Cl(5,4;5,4) and Br(5,5;5,5) [29].

The ADF atomic orbitals on Cr, Cl and Br were described by an uncontracted triple zeta Slater-type orbital basis set [30, 31] augmented by single polarisation functions. In these calculations the $1s^2 2s^2 2p^6$ configuration of both chromium and chlorine and the $1s^2 2s^2 2p^6 3s^2 3p^6 3d^{10}$ configuration of bromine were ssigned to the core and treated by the frozen core approximation [22]. A set of auxiliary *s*, *p*, *d*, *f* and *g* functions, centred on all nuclei [32], was used in order to fit electron density together with both Coulomb and exchange potentials in each SCF cycle.

2.2 The multiplet structure

The calculation of the multiplet splitting in DF theory has been discussed recently by Daul [1, 33]. Following these results, it is possible to replace the energy of a single determinant by the corresponding statistical energy as obtained in DF theory. The energy of a multiplet arising from a given configuration being, to first order, a weighted sum of single-determinantal energies, it is thus possible to obtain the multiplet splittings to the same order.

Following this line of thought we used symmetry-based arguments to rationalise the relationship between the multiplet splittings and single-determinantal energies as obtained in DF theory. A system of FORTRAN programs working on both mainframe or personal computers has been developed to obtain these relations. In the case of symmetrical molecules with degenerate orbitals, the multiplets arising from an open-shell configuration can in general no longer be expressed by a single determinant. That is, DF calculations do not yield multiplet energies directly. Instead, multiplet energies follow only after an approximate symmetry analysis. Actually, the use of symmetry will not only enable us to perform such calculations, but also to simplify the problem considerably. For more details the reader should consider Ref. [1]

3 Results and discussion

It is known that from a purely theoretical point of view that excited states are difficult to handle in DF theory because: (i) the Hohenberg Kohn theorems are in principle only valid for a canonical ensemble including the ground state and finite number of excited states [34, 35] and (ii) as it is the case also for HF based models, there is the orthogonality problem of the excited state wave function to that of the ground state [36]. However, our results show, as reported also by Daul et al. [37], that we are able with this approach to simultaneously describe the ground and excited states with similar accuracy. Hence, DF models may thus represent a valuable alternative to CI approaches to evaluate properties of excited states.

The three lowest terms of the Cr(III) free ion $3d^3$ configuration i.e. ^4F, ^4P and ^2G are reduced in an octahedral environment as follows:

$$^4F \rightarrow {}^4A_{2g} + {}^4T_{2g} + {}^4T_{1g},$$

$$^4P \rightarrow {}^4T_{1g},$$

$$^2G \rightarrow {}^2E_g + {}^2T_{1g} + {}^2T_{2g} + {}^2A_{1g}.$$

In the majority of the luminescent octahedral Cr(III) complexes, emission occurs in the form of a sharp line stemming from the excited ^2E_g state. However, a broad band near-infrared emission also occurs from the $^4T_{2g}$ state in the title compounds as a consequence of the weak crystal field induced by ligand such as Cl^- and Br^-. This yields unusual photophysical properties for this state. In particular the analysis of this emission allows one to probe the Jahn–Teller distortion of the $^4T_{2g}$. Hence, one purpose of our work was to explore the energy surface of the low-lying multiplets versus the chromium-ligand bond lengths d(Cr–L) and to determine their energy minima. The following multiplets were considered in our calculation: $|t_2^3\ {}^2E>$, $|et_2^2\ {}^4T_2>$ and $|et_2^2\ {}^4T_1>$. Their energies can be obtained as shown below from the energies of the following DFT

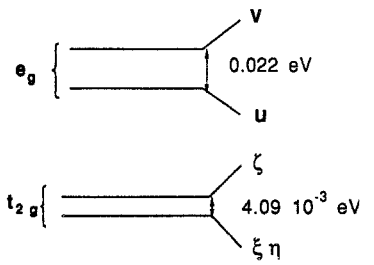

Fig. 1. Incidence of a small axial elongation on the "3*d*" electronic energy levels of $[CrCl_6]^{3-}$

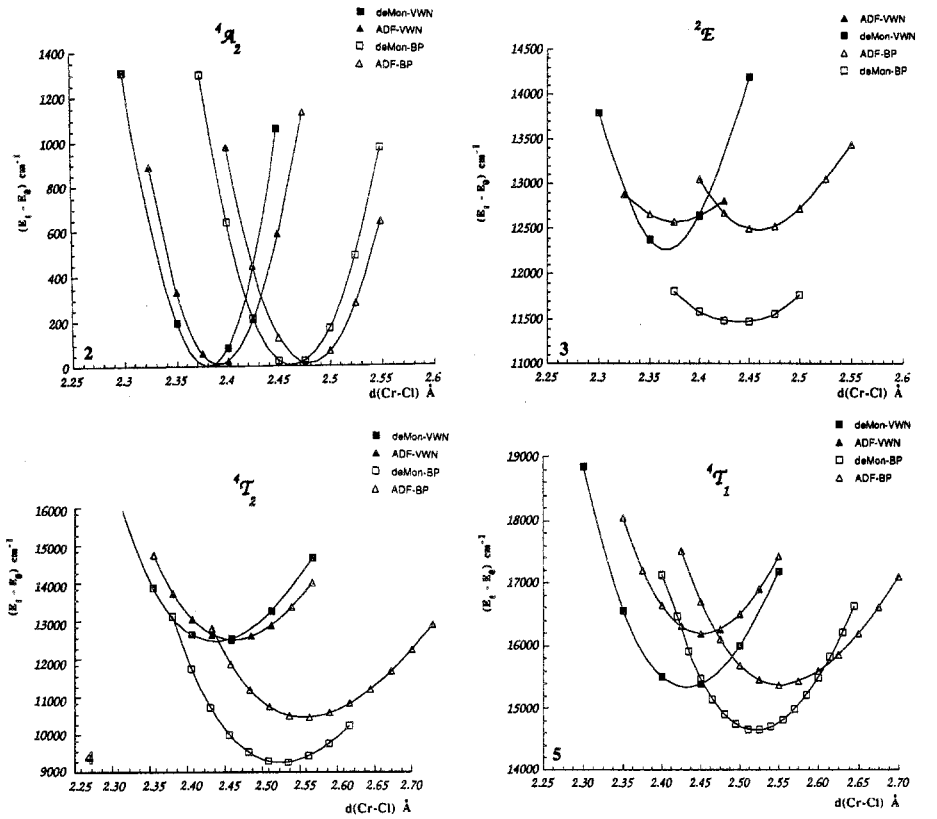

Fig. 2. Potential energy curve of the $^4A_2$ ground state of $[CrCl_6]^{3-}$ as function of d(Cr–Cl). E_0 is the energy of relaxed ground state

Fig. 3. Potential energy curve of the ^2E excited state of $[CrCl_6]^{3-}$ as function of d(Cr–Cl)

Fig. 4. Potential energy curve of the $^4T_2$ excited state of $[CrCl_6]^{3-}$ as function of d(Cr–Cl)

Fig. 5. Potential energy curve of the $^4T_1$ excited state of $[CrCl_6]^{3-}$ as function of d(Cr–Cl)

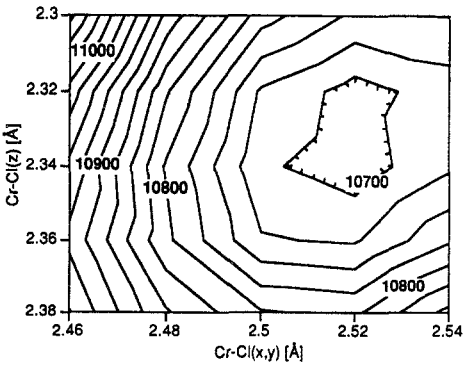

Fig. 6. $^4T_2$ isoenergies versus d(Cr–Cl(x, y)) and d(Cr–Cl(z)) using ADF VWN

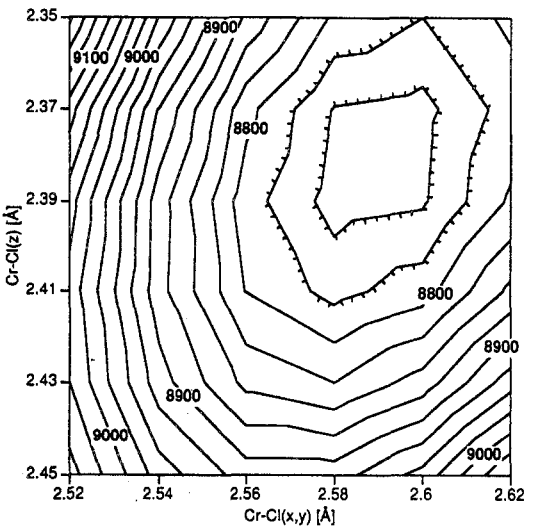

Fig. 7. Energy of $^4T_2$ isoenergies versus d(Cr–Cl(x, y)) and d(Cr–Cl(z)) using deMon including Becke–Perdew corrections

single determinants (cf. Sect. 2.2):

$$E(^4A_2) = E(|\zeta^+\eta^+\zeta^+|).$$

$$E(^4T_2) = E(|u^+\zeta\eta^+|),$$

$$E(^4T_1) = E(|v^+\zeta\eta^+|),$$

$$E(^2E) = 1.5E(|\zeta^+\eta^+\zeta^-|) - 0.5E(|\zeta^+\eta^+\zeta^+|),$$

where u and v are components of e_g and $\zeta\eta$ and ζ components of t_{2g}.

Since deMon does not use symmetry-adapted basis functions, a small axial elongation of 0.008 Å is arbitrarily used to induce a small splitting in order to identify the components of e_g and t_{2g}. This distortion has no significant incidence on the calculation (cf. Fig. 1).

The dependence of the multiplet energies upon the metal–ligand bond length d(Cr–L) is reported in Figs. 2–5 for $[CrCl_6]^{3-}$ and in Figs. 8 – 11 for $[CrBr_6]^{3-}$. These curves represent, respectively, the energies of excited states of calculations performed using both ADF and deMon programs with and without nonlocal corrections relative to the energy of the relaxed ground state.

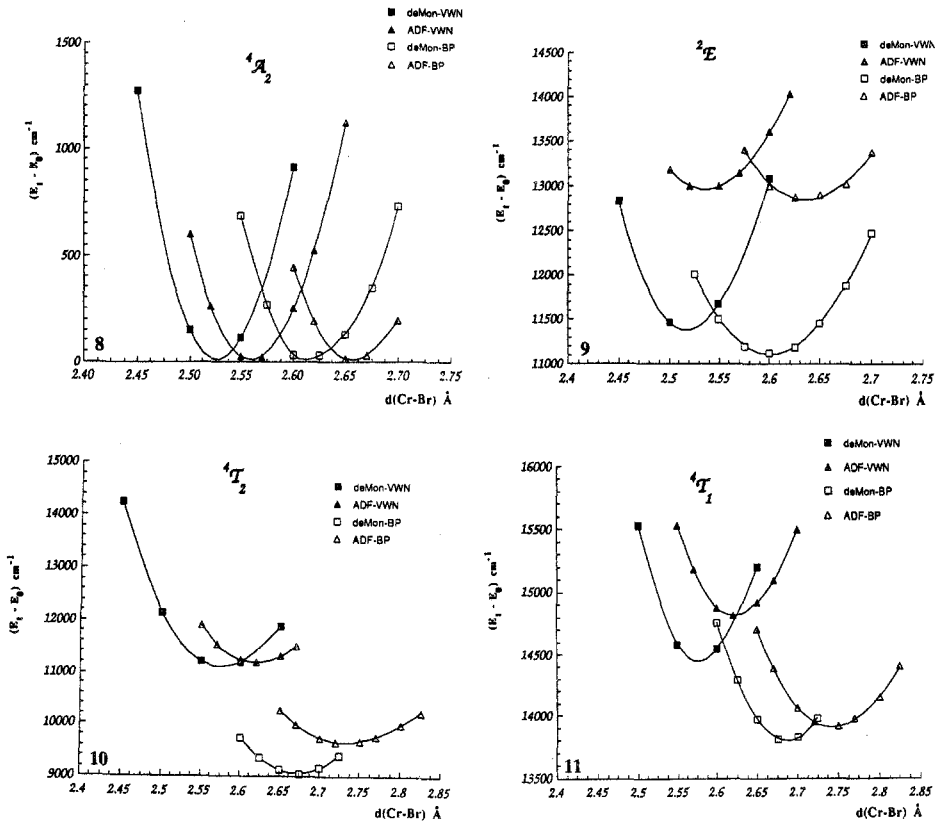

Fig. 8. Potential energy curve of the $^4A_2$ ground state of $[CrBr_6]^{3-}$ as function of d(Cr–Br)

Fig. 9. Potential energy curve of the ^2E excited state of $[CrBr_6]^{3-}$ as function of d(Cr–Br)

Fig. 10. Potential energy curve of the $^4T_2$ excited state of $[CrBr_6]^{3-}$ as function of d(Cr–Br)

Fig. 11. Potential energy curve of the $^4T_1$ excited state of $[CrBr_6]^{3-}$ as function of d(Cr–Br)

The equilibrium geometries, the absorption and emission energies and the Stokes shift for the states considered are reported in Table 1 and Table 2.

We notice that BP nonlocal gradient corrections lead to an increase of bond distances. Without these corrections bond lengths are too short. Hence these corrections are therefore important to describe accurately the geometry of such compounds. Indeed, the equilibrium bond length obtained using both deMon and ADF programs at the level of VWN approximation is underestimated when compared with the experimental value. The value of d(Cr–L) for the relaxed ground state obtained by ADF are longer (0.02 Å for Cr–Cl and 0.04 Å for Cr–Br) than the value obtained by deMon. These small deviations are probably due to the different basis sets used.

The large geometrical expansion of d(Cr–Cl) in the $^4T_2$ state can be easily understood in terms of orbital occupancies. As the excited states result from

Table 1. Comparison between experimental and calculated ground state and excited state properties of $[CrCl_6]^{3-}$

	deMon VWN[a]	deMon BP[b]	ADF VWN[c]	ADF BP[d]	Exp.
$^4A_2$ d(Cr–Cl) [Å]	2.382	2.462	2.391	2.481	2.44[h]
$^4A_2 \rightarrow {}^4T_2$					
Absorption maximum [cm^{-1}]	12550	9760	12720	10910	12658[e]
$^4T_2 \rightarrow {}^4A_2$					
Emission maximum [cm^{-1}]	11030	8382	10090	9090	10016[e]
Stokes shift [cm^{-1}]	1520	1380	2630	1820	2642[f] 1740[g]
$^4T_2$ d(Cr–Cl(x, y)) [Å]	2.492	2.592	2.521	2.635	2.54[i]
d(Cr–Cl(z)) [Å]	2.319	2.381	2.333	2.397	2.41[i]
$^4A_2 \rightarrow {}^2E$					
Absorption maximum [cm^{-1}]	12320	11509	12740	12560	14550[e]
$^4A_2 \rightarrow {}^4T_1$					
Absorption maximum [cm^{-1}]	15890	14650	16810	15980	18020[e]
Jahn–Teller energy[j] [cm^{-1}]	900	662	1400	747	310[i]
Ground state vibrational frequencies: $a\|_g$ [cm^{-1}]	236				291[i]
e_g [cm^{-1}]	164				227[i]

[a–d] See text; [e] Ref. [38]; [f] Ref. [39]; [g] Ref. [40]; [h] Ref. [41]; [i] Ref. [42]
[j] Difference between the energy of $^4T_2$ in O_h and D_{4h} symmetry

an electronic excitation to the e_g MO, which is strongly antibonding, it is not surprising that they are characterised by significant increase of Cr–L distance.

It appears that the energies of the excited states are slight;y overestimated when the nonlocal corrections are used. This behaviour is unusual and not yet well understood. Further investigations are currently in progress in order to clarify this point.

Using M–L bond lengths of the relaxed ground state, deMon calculations lead to 12550 cm^{-1} and ADF to 12700 cm^{-1} for $^4A_2$–$^4T_2$ energy difference in the VWN approximation. This is in agreement with the MSXα DF calculations of Monnier et al. which yields [44] 12000 cm^{-1} for the same transition.

In a ligand field (LF) model the energy of the $^4T_2$ excited state depends only upon 10Dq. For those cases, where the difference of electrostatic repulsion between the ground state and excited states vanishes, both DFT and HF yield good transition energies. On the other hand the correct prediction of the ^2E energy is more difficult, as it depends upon Racah parameters B and C in a LF description. The best agreement we obtain is at variance by about 2000 cm^{-1} when compared with the experimental transition energy. Using the open shell Roothaan HF method for the similar compound $[CrF_6]^{3-}$, Pierloot et al. [13] predict the energy

Table 2. Comparison between experimental and calculated ground state and excited state properties of $[CrBr_6]^{3-}$

	deMon VWN[a]	deMon BP[b]	ADF VWN[c]	ADF BP[d]	Exp.
$^4A_2$ d(Cr–Cr) [Å]	2.525	2.615	2.562	2.657	2.60[e]
$^4A_2 \rightarrow {}^4T_2$					
Absorption maximum [cm^{-1}]	11590	9500	11670	10150	13400[f]
$^4T_2 \rightarrow {}^4A_2$					
Emission maximum [cm^{-1}]	10225	8055	10030	8210	11200[f]
Stokes shift [cm^{-1}]	894	1003	1162	1438	2200[f]
$^4T_2$ d(Cr–Br(x, y)) [Å]	2.634	2.76	2.68	2.84	2.75[f]
d(Cr–Br(z)) [Å]	2.496	2.54	2.50	2.57	2.55[f]
$^4A_2 \rightarrow {}^2E$					
Absorption maximum [cm^{-1}]	12320	11509	12740	12560	13900[g]
$^4A_2 \rightarrow {}^4T_1$					
Absorption maximum [cm^{-1}]	14930	14440	15301	14583	17700[g]
Jahn–Teller energy [cm^{-1}]	469	680	642	963	
Ground state vibrational frequencies: a_{1g} [cm^{-1}]	107				183[h]
e_g [cm^{-1}]	80				144[h]

[a–e] See text; [f] Ref. [42]; [g] Ref. [43]; [h] Ref. [39]

of this state to be 5700 cm^{-1} above the experimental value. A correlation treatment with 13 electrons in the ($1t_{2g} + 3e_g$) and ($2t_{2g} + 4e_g$) orbitals allows to reduce this difference to 2200 cm^{-1}.

The $^4T_2$ state exhibits orbital degeneracy, and one does expect a Jahn–Teller deformation for this state. This predicted energy contours are reported in Figs. 6, 7 and 12, 13 which display the energy of the $^4T_2$ in function of the axial bond length d(Cr–L_z) and the equatorial bond length: d(Cr–$L_{x,y}$). We found that in all cases the system moves to a more stable geometry when the axial bond length is compressed and the equatorial one elongated. The main features of the Jahn–Teller deformation for this state are reported in Tables 1 and 2. It is seen that the deMon calculation with Becke–Perdew correction gives the best results in comparison with the experimental data.

When comparing DFT calculation performed for ruthenocene [37], and examining the present result, one may therefore deduce, that DFT methods are able to describe both ground and excited states.

The Jahn–Teller energies, i.e. the difference between the energy of $^4T_2$ in O_h and D_{4h} symmetry, are overestimated. This might be due to the fact that we did perform cluster calculations which does not take into account the bulk of the lattice host. Madelung corrections due to the host lattice are currently in progress in our laboratories.

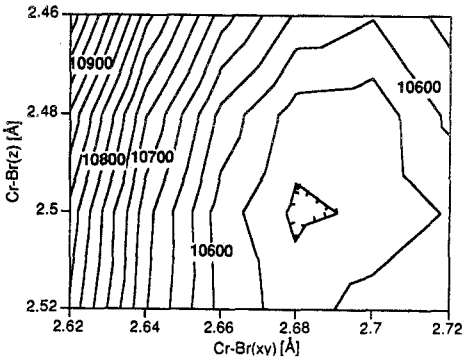

Fig. 12. $^4T_2$ isoenergies versus d(Cr–Br(x, y)) and d(Cr–Br(z)) using ADF VWN

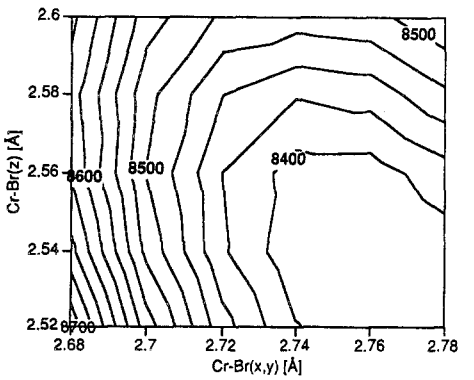

Fig. 13. $^4T_2$ isoenergies versus d(Cr–Br(x, y)) and d(Cr–Br(z)) using deMon including Becke–Perdew corrections

Acknowledgements. The authors are grateful to Prof. D.R. Salahub and to Prof. E.J. Baerends for providing copies of their DFT programs and for fruitful discussions. Financial support by the Swiss National Science Foundation and the Federal Office for Education and Science, acting as Swiss COST Office, is gratefully acknowledged.

References

1. Daul C (1994) Int J Quantum Chem 52:867
2. Bellafrouh K, Daul C, Michel-Calendini FM (1992) New J Chem 16:1123
3. Michel-Calendini FM, Bellafrouh K, Daul C (1992) Ferroelectrics 125:271
4. Griffith JS (1971) The theory of transition metal ions, Cambridge University Press, Cambridge
5. Slater JC (1972) Adv Quantum Chem 6:1
6. Richardson FS, Reid MF, Dallara JJ, Smith RR (1985) J Chem Phys 83:3813
7. Tanner PA (1985) J Chem Phys 85:3813
8. Kenyon PT, Andrews, L McCollum B, Lempicki A (1982) IEEE J Quant Electron QE18
9. Florez M, Seijo L, Pueyo L (1986) Phys Rev B 34:1200
10. Carsky R, Dedieu A (1986) Chem Phys 103:265
11. Vanquickenborne LG, Hendrickx M, Postelmans D, Hyla-Kryspin I, Pierloot K (1988) Inorg Chem 27:900
12. Pierloot K, Verhulst J, Verbeke P, Vanquickenborne LG (1989) Inorg Chem 28:3059
13. Pierloot K, Vanquickenborne LG (1990) J Chem Phys 93:4154
14. Larson S, Roos BO, Siegbahn PEM (1983) Chem Phys Lett 96:436
15. Veillard A, Strich A, Daniel C, Siegbahn PEM (1987) J Chem Phys Lett 141:329

16. Jahn HA, Teller E (1937) Proc R Soc London Sect A 161:220; Jahn HA (1937) Proc R Soc London Sect A 164:117
17. Andzelm J, Radzio E, Salahub DR (1985) J Chem Phys 83:4573
18. Salahub DR (1986) In: Smith VH, Schaefer HF, Morokuma K (eds) Applied quantum chemistry. Reidel, Dordrecht, p 185
19. Salahub DR (1987) Adv Chem Phys 69:447
20. Salahub DR, Fournier R, Mlynarski P, Papai I, St-Amant A, Ushio J (1991) In: Labanowski JK, Andzelm JW (eds) Denisty functional methods in chemistry. Springer, New York, p 77
21. Baerends EJ, Ellis DE, Ros P (1971) Chem Phys 2:41
22. Ravenek W (1987) In: te Riele HJJ, Dekker ThJ, van de Vorst HA (eds) Algorithms and applications on vector and parallel computers. Elsevier, Amsterdam
23. Boerrigter PM, Te Velde G, Baerends EJ (1988) Int J Chem Quantum Chem 33:87
24. Te Velde G, Baerends EJ (1992) J Comput Phys 99:84
25. Vosko HS, Wilk L, Nusair N (1980) Can J Phys 58:1200
26. Perdew JP (1986) Phys Rev B33:8822; B34:7046
27. Becke AD (1988) J Chem Phys 88:2457
28. Becke AD (1988) Phys Rev A38:3098
29. Godbout N, Andzelm J, to be published
30. Snijders GJ, Baerends EJ, Vernooijs P (1982) Atomic Nucl Data Tables 26:483
31. Snijders GJ, Baerends EJ, Vernooijs P (1981) In: Slater type basis functions for the whole periodic system internal report. Free University of Amsterdam, Netherlands
32. Krijn J, Baerends EJ (1984) In: Fit functions in the HFS-methods internal report. Free University of Amsterdam, Netherlands
33. Daul C (1989) J Chim Phys 86:703
34. Hohenberg P, Kohn W (1964) Phys Rev A 136:864
35. Kohn W, Sham LJ (1964) Phys Rev A 140
36. Parr RG, Yang W (1989) Density functional theory of atoms and molecules. Oxford University Press, New York
37. Daul C, Güdel HU, Weber J (1993) J Chem Phys 98:4023
38. Andrews LJ, Lempicki A, McCollunm BC, Giunta CJ (1986) Phys Rev B 34:2735
39. Woods AM, Sinkovits RS, Charpie JC, Huang WL, Bartram RH, Rossi AR (1993) J Phys Chem Solids N5 54:543
40. Veillard A, Demuynk J (1987) In: Schaeffer HF (ed) Modern theoretical chemistry, Vol 4, p 187
41. Reber C, Güdel HU, Meyer G, Schleid T, Daul C (1989) Inorg Chem 28:3249
42. Knochenmuss R, Reber C, Rajasekharan MV, Güdel HU (1986) J Chem Phys 85:4280
43. Lever ABP (1984) Inorganic electronic spectroscopy. Elsevier, Amsterdam
44. Monnier A, Chambaz D, Bill H, Weber J (1989) J Chem Phys 91:6650
45. Jungwirth P, Stussi D, Weber J (1992) Chem Phys Lett 190:29